ARTIFICIAL SATELLITES, Vol. 49, No. 2 – 2014
DOI: 10.2478/arsa-2014-0007

SIMPLIFIED ORBIT DETERMINATION ALGORITHM FOR LOW EARTH ORBIT SATELLITES USING SPACEBORNE GPS NAVIGATION SENSOR

Sandip Tukaram Aghav, Shashikala Achyut Gangal
Department of Electronic Science, University of Pune, Pune, India,
sandip.aqua@gmail.com

ABSTRACT

In this paper, the main work is focused on designing and simplifying the orbit determination algorithm which will be used for Low Earth Orbit (LEO) navigation. The various data processing algorithms, state estimation algorithms and modeling forces were studied in detail, and simplified algorithm is selected to reduce hardware burden and computational cost. This is done by using raw navigation solution provided by GPS Navigation sensor. A fixed step-size Runge-Kutta 4^{th} order numerical integration method is selected for orbit propagation. Both, the least square and Extended Kalman Filter (EKF) orbit estimation algorithms are developed and the results of the same are compared with each other. EKF algorithm converges faster than least square algorithm. EKF algorithm satisfies the criterions of low computation burden which is required for autonomous orbit determination. Simple static force models also feasible to reduce the hardware burden and computational cost.

Keywords: GPS Navigation Sensor, atmospheric drag, extended Kalman filter.

1. INTRODUCTION

Orbit determination is the process of determining the best estimate of the state of a spacecraft, whose initial state is unknown, from observations influenced by random and systematic errors, using a mathematical model that is not exact. In this work above-mentioned procedure will be referred to as the orbit determination (Taply et al., 2004). There are various techniques available for satellite position measurement at given epoch time. These include *one way* technique which is based on the transmittal of a signal by a satellite or ground-based transmitter that is received by a separate instrumentation. The transmitted signal propagates along a path and arrives at a point instrumented to receive the transmitted signal. This way one can calculate range and range rate between two points. In *two way* method it uses both uplink and downlink path to calculate the range and range rate. Satellites Laser Ranging (SLR) technique comes under two way method. However ground based tracking carries extensive cost burden in spacecraft mission. In order to make the satellite orbit control system autonomous and reduce the need for ground intervention there is a need for on-board availability of continuous and accurate knowledge of the satellite

orbit. From this information, position and velocity vector of an orbiting LEO spacecraft is determined as a function of time (Parkinson and Spilker, 1996). The measurement principle in its simplest form is illustrated by Fig. 1 where $\rho_j, \rho_k, \rho_l, \rho_m$ are the pseudoranges of the respective GPS satellites and $r(t)$ is the geocentric distance of LEO. Each GPS satellite sends its own positional information in the form of navigation data. The code measurements of at least four GPS satellite observed at observation time t by the on-board GPS navigation sensor, are used to determine geocentric position vector $\vec{r}(t)$ of the LEO's centre of mass.

An efficient Low Earth Orbit (LEO) precise orbit determination algorithm has presented by (Bock et al., 2002). They used IGS orbits and precise clocks for the GPS satellites and the positions are generated by the combination of code derived positions and phase derived position differences. Fitting an orbit based on a physical model to the positions promises to complement a procedure that meets the requirements regarding precision and processing speed. The positions estimated from code observations and position differences estimated from phase observations may eventually be used as "pseudo-observations" to fit an orbit based on the physical model using a least squares adjustment. A new onboard orbit determination algorithm based on the unscented Kalman filter (UKF) has been successfully developed by (Choi et al., 2010) for application to spaceborne GPS receivers. The perturbations due to 40x40 geopotential, the gravity of the Sun and Moon, atmospheric drag, and solar radiation pressure were employed to develop the precision orbit propagation for onboard processing. The 7(8)th-order Runge–Kutta numerical integration was applied for orbit propagation. The Cowell method was applied for modeling orbit motion. Researcher (Pardal et al., 2009) determined the orbit of an artificial satellite and analyzed its implications, using least squares algorithms through sequential given rotations as the method of estimation, and data of the GPS receivers. In this paper, an algorithm to determine onboard the satellite orbit in real-time using the GPS system and Kalman filtering is developed. It used a simplified and compact model with low computational cost. The extended Kalman filter (EKF) estimates the state vector, composed of the position and velocity components, bias, drift, and drift rate of the GPS receiver clock. An algorithm for real-time and onboard orbit determination applying the Extended Kalman Filter (EKF) method is developed by (Chiaradia et al., 2013). The minimum set of to-be-estimated states to reach the level of accuracy of tens of meters is found to have at least the position, velocity, and user clock offset components. The dynamical model is assessed through several tests, covering force model, numerical integration scheme and step size, and simplified variational equations. The measurement model includes only relevant effects to the order of meters. Based on the same principle a simple but fairly accurate algorithm is developed to determine the LEO satellite's orbit using raw navigation solution provided by GPS navigation sensor.

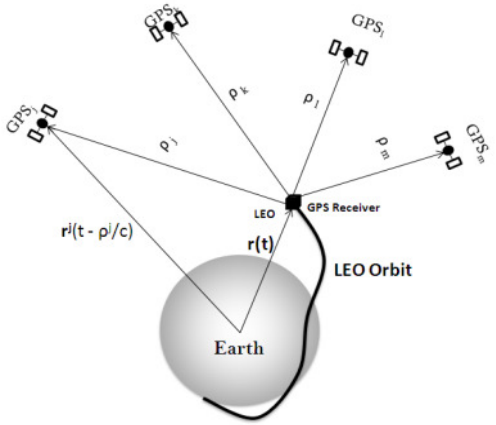

Figure 1. Concept of Autonomous Orbit determination

2. METHODOLOGY

For determining initial orbit, one should know the position of satellite in an orbit w. r. t. the elapsed time, $t - t_0$, or conversely, how long it takes to go from one point in an orbit to another. To solve this, Kepler introduced the quantity M, called the mean anomaly, which is the fraction of an orbit period that has elapsed since perigee as given in Eq. (1). The mean anomaly equals the true anomaly for a circular orbit.

$$M - M_0 = n(t - t_0) \tag{1}$$

where, M_0 is the mean anomaly at time t_0 and n is the mean motion, or the average angular velocity determined from the semi-major axis a of the orbit as given in Eq. (2);

$$\mathrm{n} = \sqrt{\frac{\mathrm{GM}}{\mathrm{a}^3}} \qquad GM = \text{Product of gravitational constant and mass of the body} \tag{2}$$

Mean anomaly is a function of eccentric anomaly (E) given in the Eq. (3);

$$M = E - e \sin E \qquad \text{where, e is orbital eccentricity} \tag{3}$$

At any time in its orbit, the magnitude of a spacecraft's position vector, i.e. its distance from the primary body (r), latitude of the satellite (θ) and longitude of the satellite (ϕ) can be calculated from the following Eq. (4);

$$r = \frac{a(1 - e^2)}{1 + ecosv}$$
$$\theta = \sin^{-1}[\sin i \ \sin v] \tag{4}$$
$$\phi = \sin^{-1}\left[\frac{\tan\theta}{\tan i}\right]$$

where, i, θ, v are inclination angle, latitude and true anomaly of the satellite, length ϕ refers to a prime meridian specified in the inertial reference frame of the standard epoch J2000.0.

From (r, θ, ϕ) of the satellite, position vector components x, y, z in Cartesian coordinate system as a function of time (t) is obtained from Eq. (5) as follows;

$$x = r\cos\theta \ \cos\phi$$
$$y = r\cos\theta \ \sin\phi \tag{5}$$
$$z = r\sin\phi$$

Then $\vec{r}(t) = x(t)\vec{\imath} + y(t)\vec{\jmath} + z(t)\vec{k}$ is the position vector of the satellite and the magnitude of $\vec{r}$ is $\sqrt{x^2 + y^2 + y^2}$.

The perturbations due to the factor J_2 (flattening coefficient of the Earth) is only considered for determining the reference orbit from initial measurements. Longitude of ascending node, argument of

perigee and mean motion are mostly affected. The factor J_2 is the flattening coefficient of the Earth and is equal to 0.0010827 (Parkinson and Spilker, 1996).

The accuracy of the orbital elements is directly dependent upon the accuracy of velocity vector components. To determine position components as a function of time, the velocity vector components are numerically integrated. In the present paper, the acceleration vectors are numerically integrated with the help of fixed step size 4th order Runge-Kutta method for finding out the velocity vector components (Parkinson and Spilker, 1996).

2.1. Numerical integration of the equation of motion

The satellite dynamic model used for the satellite orbit propagation is given in Eq. (6);

$$\ddot{\vec{r}}(t) = \frac{\mu}{r^3}\vec{r}(t) + \vec{w}(t) \tag{6}$$

where, $\ddot{\vec{r}}(t)$ is the acceleration vector, $\vec{r}(t)$ is the orbital position vector and $\vec{w}(t)$ is vector of the process noise, which is assumed to be zero for calculation simplicity. The discrete-time measurements which are considered for the present study include position and velocity vector obtained from *Oceansat2* GPS navigation sensor.

The zonal perturbations J_2, J_3 and J_4 are considered for simulations. The main deviation from central gravitational field is caused by dynamic flattening of the Earth. In the Geodetic Reference System 1980 (GRS80), normal field of the flattening coefficient is represented by term J_2= 0.001082. Similarly higher order flattening coefficients J_3 and J_4 are given as J_3= -0.0000025323 and J_4= -0.0000016204 (Parkinson and Spilker, 1996).

The acceleration components $\ddot{x}$, $\ddot{y}$and $\ddot{z}$ of satellite dynamic model with term J_2 are given in Eq. (7) as discussed in (Zarchan, 2005, Vallado and McClain, 2007);

$$\ddot{x} = \frac{-\mu x}{r^3}\left[1 + J_2\left(\frac{R_e}{r}\right)^2\frac{3}{2}\left(1 - 5\frac{z^2}{r^2}\right) + J_3\left(\frac{R_e}{r}\right)^3\frac{5}{2}\left(3 - 7\frac{z^2}{r^2}\right)\frac{z}{r} - J_4\left(\frac{R_e}{r}\right)^4\frac{5}{8}\left(3 - 42\frac{z^2}{r^2} + 63\frac{z^4}{r^4}\right)\right]$$

$$\ddot{y} = \frac{-\mu y}{r^3}\left[1 + J_2\left(\frac{R_e}{r}\right)^2\frac{3}{2}\left(1 - 5\frac{z^2}{r^2}\right) + J_3\left(\frac{R_e}{r}\right)^3\frac{5}{2}\left(3 - 7\frac{z^2}{r^2}\right)\frac{z}{r} - J_4\left(\frac{R_e}{r}\right)^4\frac{5}{8}\left(3 - 42\frac{z^2}{r^2} + 63\frac{z^4}{r^4}\right)\right] \tag{7}$$

$$\ddot{z} = \frac{-\mu z}{r^3}\left[1 + J_2\left(\frac{R_e}{r}\right)^2\frac{3}{2}\left(3 - 5\frac{z^2}{r^2}\right) + J_3\left(\frac{R_e}{r}\right)^3\frac{5}{2}\left(6 - 7\frac{z^2}{r^2}\right)\frac{z}{r}\right] + \frac{\mu}{r^2}J_3\left(\frac{R_e}{r}\right)^3\frac{3}{2} + \frac{\mu z}{r^3}J_4\left(\frac{R_e}{r}\right)^4\frac{5}{8}\left(15 - 70\frac{z^2}{r^2} + 63\frac{z^4}{r^4}\right)$$

where, μ is the earth gravitational constant, R_e is the Earth's radius, and r is the magnitude of position vector. To update the state vector, Eq. (7) is numerically integrated using Runge-Kutta 4th order fixed step size method. Least square differential correction and EKF are used to generate the optimal state estimates of the satellite orbit.

Atmospheric drag is the third most dominant force acting on a low Earth orbiting satellite (depending on the altitude in low Earth orbit), after the forces due to central body and oblateness of the Earth. For satellites orbiting at higher altitudes, radiation pressure due to the Sun as well as third body effects becomes

significant and dominant as well. Apart from the undesirable effects of satellite drag, other applications such as aerobraking and space tethers require an accurate model of the atmosphere for high accuracy solutions. The three main areas under which drag is studied are for orbit determination under the influence of drag, satellite lifetime estimation, and to determine the physical properties of the upper atmosphere.

When a satellite encounters atmospheric molecules, it experiences a retarding force, the drag force, due to momentum transfer from the latter. This results in a loss of energy of the satellite and thus drag is a non-conservative force. Other non-conservative forces acting on the satellite include the radiation forces due to the Sun, Earth albedo, and Earth infrared. The effect of the drag is to reduce the semimajor axis (due to loss of energy) and the eccentricity (making it less elliptical). Other orbital elements are also affected by drag but the effects are periodic in nature. Drag also results in some coupling effects with the aspherical potential.

The need for a rigorous model of the effects of atmospheric perturbations requires knowledge in the fields of molecular chemistry, thermodynamics, aerodynamics, hypersonics, meteorology, electro-magnetics, planetary science, and orbital mechanics. Thus, study of astrodynamics in the presence of the atmosphere is very difficult. Nevertheless, accurate determination of atmospheric properties is essential for satellite drag studies (Degnan and Pavlis, 1994).

The acceleration experienced by a satellite is given by the following Eq. (8) which relates the acceleration with atmospheric properties, geometrical properties of the satellite, and the relative velocity vector of the satellite.

$$\vec{a}_{drag} = -\frac{1}{2}\frac{C_D A}{m}\rho v_{rel}^2 \frac{\vec{v}_{rel}}{|\vec{v}_{rel}|} \tag{8}$$

The first quantity in the above drag equation C_D is the coefficient of drag, a dimensionless quantity which quantifies the resistance of a body. C_D, depends on the temperature and composition of the surrounding atmosphere, surface properties of the satellite including its temperature, surface geometry, and orientation. The drag coefficient for a flat plate is about 2.2 and about 2.0 to 2.1 for spheres, in the upper atmosphere (Amaral et al, 2007). C_D is usually estimated up to three significant digits. ρ is the atmospheric density, which is the hardest to estimate. Several atmospheric models exist which are used to estimate neutral density, whose details will be discussed in future sections. A is the cross sectional area that is normal to the velocity vector. For a satellite whose attitude and geometry are known, determining A may be relatively easy. However, if the attitude of an aspherical satellite is not known, then determining the cross sectional area becomes difficult, especially if the satellite's attitude is rapidly changing, say a tumbling satellite. m is the mass of the satellite. The mass may be constant or changing during the mission depending on whether the onboard propellants (if any) are being consumed. $\vec{v}_{rel}$ is the velocity vector of the satellite relative to the atmosphere and v_{rel} is its magnitude.

The quantity $C_D A/m$ is called the ballistic coefficient (BC) is another measure of a satellite susceptibility to drag. Higher BC means lower drag is experienced by the satellite. The atmosphere is not stationary in the inertial frame but rotates with the Earth. However, the rotational rate is not the same as that of the Earth at higher altitudes but rather rotates with a profile; so the layer next to the surface has the same rotational speed as that of the Earth, and the ones above gradually decrease in speed. Often, this lag is ignored and the atmosphere layer at the satellite altitude is assumed to rotate at the same rate as the surface of the Earth. Using this approximation, the expression for the relative velocity of the satellite in the inertial frame is given in Eq. (9).

$$\vec{v}_{rel} = \frac{d\vec{r}}{dt} - \vec{\omega}_{\oplus} \times \vec{r} = \begin{bmatrix} \frac{dx}{dt} + \omega_{\oplus} y & \frac{dy}{dt} - \omega_{\oplus} x & \frac{dz}{dt} \end{bmatrix}^T \tag{9}$$

In the above equation, $\vec{r}$ is satellite position vector with $x, y,$ and z components, $\vec{\omega}_{\oplus}$ is the angular velocity vector of the Earth and $\omega_{\oplus}$ is its magnitude.

2.2. Simplified atmospheric density model

Purpose of present research was focused on to select the simplified atmospheric density model which will be suitable for hardware implementation. There are various upper atmospheric models are in use like, CIRA-72, CIRA-86, Jacchia-71, Jacchia-77, MISS-86, MISS-90, and DTM-90. However all are very complicated numerical methods and depends upon daily or monthly Sun flux and geomagnetic data which is not suitable for onboard processing. Due to these reasons the simplified analytical atmospheric density model is selected for present research. The details of the simplified analytical atmospheric density model are given in following paragraphs.

If the balanced atmosphere is considered, according to hydrostatics the density distribution is approximately a form of exponential given in Eq. (10)):

$$\rho = \rho_0 e^{[-(h_{ellp}-h_0)/H]} \tag{10}$$

Where ρ_0 is the atmospheric density of the reference spherical surface at $h_{ellp} = h_0$, h_{ellp} is the altitude measured from Earth's surface, h_0 is the base altitude, and H is the scale height at base altitude. Table 1 explains the calculated values of ρ_0 with respect to the altitude measured from earth surface (Yunck et al., 1994).

Table 1: (Part one): Nominal density (ρ_0) with respect to the altitude measures from earth surface

Altitude measured from Earth Surface (h_{ellp}) [km]	Base Altitude(h_0) [km]	Nominal density (ρ_0) [kg/m^3]	Scale Height (H) at base altitude [km]
0-25	0.00	1.23	7.25
25-30	25.00	3.899*10^-2	6.35
30-40	30.00	1.774*10^-2	6.68
40-50	40.00	3.972*10^-3	7.55
50-60	50.00	1.057*10^-3	8.38
60-70	60.00	3.206*10^-4	7.71
70-80	70.00	8.770*10^-5	6.55
80-90	80.00	1.905*10^-5	5.80
90-100	90.00	3.396*10^-6	5.38
100-110	100.00	5.297*10^-7	5.88
110-120	110.00	9.661*10^-8	7.26
120-130	120.00	2.438*10^-8	9.47
130-140	130.00	8.484*10^-9	12.64
140-150	140.00	3.845*10^-9	16.15
150-180	150.00	2.070*10^-9	22.52
180-200	180.00	5.464*10^-10	29.74
200-250	200.00	2.789*10^-10	37.11
250-300	250.00	7.248*10^-11	45.55
300-350	300.00	2.418*10^-11	53.63
350-400	350.00	9.518*10^-12	53.30

Table 1: (Part two): Nominal density (ρ_0) with respect to the altitude measures from earth surface

Altitude measured from Earth Surface (h_{ellp}) [km]	Base Altitude(h_0) [km]	Nominal density (ρ_0) [kg/m^3]	Scale Height (H) at base altitude [km]
400-450	400.00	3.725*10^-12	58.52
450-500	450.00	1.585*10^-12	60.83
500-600	500.00	6.967*10^-13	63.82
600-700	600.00	1.454*10^-13	71.84
700-800	700.00	3.614*10^-14	88.67
800-900	800.00	1.170*10^-14	124.64
900-1000	900.00	5.245*10^-15	181.05
1000-	1000.00	3.019*10^-15	268.00

2.3.Effect of Atmospheric drag

With the values mentioned in the Table 1 the atmospheric density (ρ) is calculated with the help of Eq. (10). These atmospheric density values are then future used to calculate the acceleration vector due to atmospheric drag coefficient using Eq. (8). To see combined effect of the J_2 and atmospheric drag, the Eq. (7) is modified to Eq. (11);

$$\ddot{x} = \frac{-\mu x}{r^3}\left[1 + J_2\frac{3}{2}\left(\frac{R_e}{r}\right)^2\left(1 - 5\frac{z^2}{r^2}\right)\right] + a_{drag\_x}$$
$$\ddot{y} = \frac{-\mu y}{r^3}\left[1 + J_2\frac{3}{2}\left(\frac{R_e}{r}\right)^2\left(1 - 5\frac{z^2}{r^2}\right)\right] + a_{drag\_y} \quad (11)$$
$$\ddot{z} = \frac{-\mu z}{r^3}\left[1 + J_2\frac{3}{2}\left(\frac{R_e}{r}\right)^2\left(3 - 5\frac{z^2}{r^2}\right)\right] + a_{drag\_z}$$

a_{drag_x}, a_{drag_y}, and a_{drag_z} are the $x, y,$ and z components of the acceleration vector generated by atmospheric drag.

Equations (11) which represents the equations of motion of satellite with J_2 and atmospheric drag are then numerically integrated using Runge-Kutta 4th Order numerical integration method. Code for the same is written in MATLAB.

2.4. Calculation of Orbital Elements from position and velocity vector

Numerical integration of equation of motion gives the instantaneous position vector and velocity vector (i.e. state vector) with respect to time. With the help of state vector data, the instantaneous orbital elements are calculated (Grewal et al.,2007). The details of orbital elements calculations are given below;

i. Semi-major axis(a)

Semi-major axis of an orbit is calculated using Eq. (12)

$$a = \frac{\mu}{\frac{2\mu}{r} - v^2}$$, where r and v is a magnitude of position and velocity vector respectively (12)

ii. Eccentricity vector ($\vec{e}$)

Eccentricity vector, which norm is equal to orbit eccentricity e, is calculated using Eq. (13)

$$\vec{e} = \frac{1}{\mu}\left[\left(v^2 - \frac{\mu}{r}\right)\vec{r} - (\vec{r} \cdot \vec{v})\vec{v}\right]$$, where $\vec{r}$ and $\vec{v}$ is a position and velocity vector respectively, '·' is a symbol of dot product (13)

iii. Orbit Inclination (i)

Orbit Inclination is calculated using Eq. (14)

$$i = \cos^{-1}\frac{(\vec{k} \cdot \vec{l})}{\|\vec{l}\|}$$, where $\vec{k}$ is unit vector and $\vec{l} = \vec{r} \times \vec{v}$, is angular momentum. (14)

iv. Argument of Perigee (ω)

Argument of Perigee is calculated using Eq. (15)

$$\omega = \frac{\vec{n} \cdot \vec{e}}{|\vec{n}\vec{e}|}$$, where $\vec{n} = \frac{(\vec{k} \times \vec{l})}{\|\vec{l}\|}$ is node vector and $\vec{e}$ is eccentricity vector, $\vec{k}$ is unit vector (15)

v. Longitude of ascending node (Ω)

Longitude of ascending node is calculated using Eq. (16)

$$\Omega = \cos^{-1}\left[\frac{n_x}{|\vec{n}|}\right]$$, where n_x is a x component of node vector. (16)

vi. True anomaly (υ)

True anomaly is calculated using Eq. (17)

$$\upsilon = \cos^{-1}\left(\left[\frac{1}{e}\left(\frac{a(1-e^2)}{r} - 1\right)\right]\right)$$ (17)

With the help of above formulae (Eq. 12 to Eq. 17) the six orbital elements *(a, e, i,* Ω*, ω* and *υ)* are calculated. A software routine for the same is developed in MATLAB.

2.5. Least square implementation

The basic principle of the method of least-squares is that the best estimate of the state is the estimate which minimizes the sum of the squares of the residuals. The satellite dynamic model used is given in Eq. (7). The measurement model used in this process is given in Eq. (18);

$$\vec{z}_k = \vec{h}_k\left(\vec{\boldsymbol{x}}(t_k)\right) + \vec{v}_k \qquad k=1, 2, 3.... \tag{18}$$

Where, $\vec{z}_k$, is the vector of measurements, $\vec{\boldsymbol{x}}(t_k)$ is the state vector of the system, $\vec{h}_k$, differentiable function and $\vec{v}_k$ is the measurement noise vector.
The residual is defined as given in Eq. (19)

$$\vec{v}_k = \vec{z}_k - \vec{h}_k(\vec{\boldsymbol{x}}(t_k)) \tag{19}$$

The measurement matrix for the same is calculated from Eq. (20),

$$\mathrm{H_k} = \left[\frac{\partial\overrightarrow{h_k}(\vec{\boldsymbol{x}}(t_k), t_k)}{\partial(\vec{\boldsymbol{x}}(t_k))}\right]_{\vec{\boldsymbol{x}}(t_k)=\vec{\boldsymbol{x}}_{k/k-1}} \tag{20}$$

$\mathrm{H_k}$ is the measurement information matrix also known as Jacobian matrix, $\vec{\boldsymbol{x}}_{k/k-1}$ is the state from *k-1* to k^{th} time instant.

The state transition matrix ($\phi_{k,k-1}$) is used to propagate covariance matrix is given by Eq. (21), (Grewal et al., 2007, Gomes et al., 2007);

$$\phi_{k,k-1} \approx I + F(t_{k-1})^{\mathrm{T}} \tag{21}$$

Where $F(t_{k-1}) = \begin{bmatrix} 0_{3\times3} & I_{3\times3} \\ J_{3\times3} & 0_{3\times3} \end{bmatrix}$ and 'T' denotes the matrix transpose.

Where, $J_{3\times3}$ is Jacobian coefficient matrix given in Eq. (22).

$$J_{3\times3} = \begin{bmatrix} 3\mu x^2 r^{-5} - \mu r^{-3} & 3\mu xyr^{-5} & 3\mu xzr^{-5} \\ 3\mu yxr^{-5} & 3\mu y^2 r^{-5} - \mu r^{-3} & 3\mu yzr^{-5} \\ 3\mu zxr^{-5} & 3\mu zyr^{-5} & 3\mu z^2 r^{-5} - \mu r^{-3} \end{bmatrix} \tag{22}$$

In least square differential correction approach, the epoch (reference point from which time is measured) state estimate is computed after processing full set of measurements (Xu, 2007). Due to non-linear relation between the epoch state vector and the modeled measurement, multiple iterations are required to compute

epoch state estimate. This increases hardware storage capacity requirements. Due to this fact, the system hardware carries unnecessary computational as well as power budget burden.

2.6. EKF implementation

To avoid computational as well as power budget burden, EKF method is selected for orbit estimation due to its recursive in nature (Grewal et al., 2007). It uses sequential process to update the estimates with new measurement. Flow chart for EKF based orbit estimation is shown in Fig.2. To implement EKF some initial assumptions are needed to fulfill the filter's requirement. To start the EKF process, it requires initial state estimate and initial state error covariance matrix. The initial state vector $\vec{\boldsymbol{x}}(t_0)$ of the satellite dynamic model is given by Eq. (23);

$$\vec{\boldsymbol{x}}(t_0) = [x \;\; y \;\; z \; v_x \;\; v_y \; v_z]_{\,6\times1}; \tag{23}$$

The state vector $\vec{\boldsymbol{x}}(t_0)$ includes satellite position and velocity vectors.

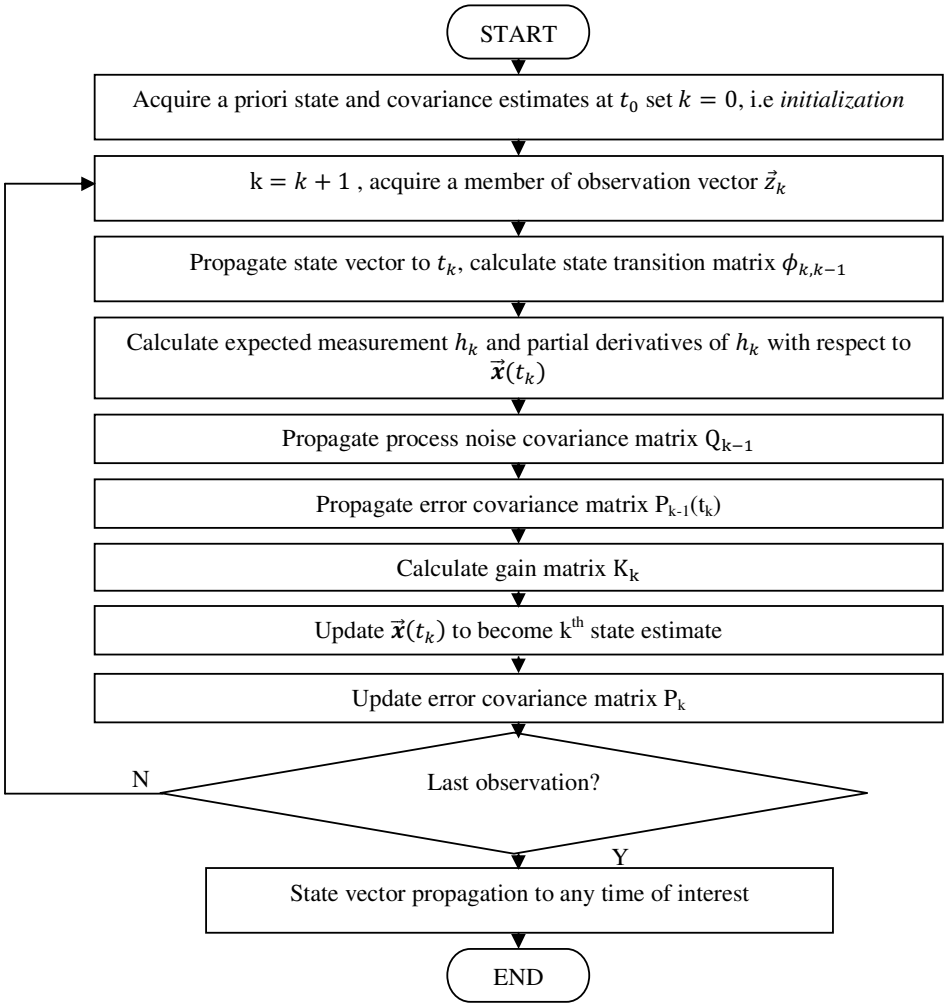

Figure 2. Flow chart for EKF based orbit estimation

A diagonal apriori covariance matrix P_{k-1} with standard deviations (σ) of 10 m (position), 0.1 m/s (velocity), is assumed. With these assumptions the apriori covariance matrix P_{k-1} is given by Eq. (24);

$$P_{k-1} = diag[\sigma_x^2 \ \sigma_y^2 \ \sigma_z^2 \ \sigma_{v_x}^2 \ \sigma_{v_y}^2 \ \sigma_{v_z}^2]_{6\times6} \tag{24}$$

To cope with deficiencies of the employed propagation model, a fixed diagonal process noise matrix Q_{k-1} is considered in the time update of the covariance matrix as given in Eq. (25);

$$P_{k/k-1} = \phi_{k,k-1} P_{k-1} \phi^T{}_{k,k-1} + Q_{k-1} \tag{25}$$

Representative process noise values used in the present application are $(10^{-3}\text{m})^2$ (position), $(10^{-6}$ m/s$)^2$ (velocity).

The state transition matrix ($\phi_{k,k-1}$) shown in Eq. (25) is computed. The actual measurements are collected from GPS Navigation sensor and modeled using Eq. (18). With the help of $P_{k/k-1}, H_k$ and R_k parameters Kalman gain K_k is calculated using the Eq. (26),

$$K_k = P_{k/k-1} H_k^T \left[H_k P_{k/k-1} H_k^T + R_k\right]^{-1} \tag{26}$$

The Kalman Gain is used as feedback for correcting state estimates, R_k is measurement noise covariance matrix which is in general a Gaussian zero-mean noise and the correction vector $\delta\vec{\hat{x}}_k$ is obtained from Eq. (27);

$$\delta\vec{\hat{x}}_k = K_k \left\{\vec{z}_k - \vec{h}_k\left(\vec{\hat{x}}_{k/k-1}\right)\right\} \tag{27}$$

And new predicted error covariance P_k is obtained from Eq. (28);

$$P_k = (I - K_k H_k) P_{k/k-1} (I - K_k H_k)^T + K_k R_k K_k^T \tag{28}$$

In this approach, EKF processes a single scalar or vector measurement at a time and yields sequential state estimate at the measurement times.

2.7. GPS data processing

There are two types of GPS codes which are transmitted by the GPS satellite vehicle. One of them (P-code) provides precise positioning with an accuracy of approximately few tens of meters. This code can only be used by a receiver with access to the encryption key. This code is only for military users. The second code is available to any commercial user. This code is known as Coarse/Acquisition (C/A) code. This code is discussed here.

Each satellite transmits two carrier signals. One is centered at 1575. 42 MHz (known as L1 carrier) uses Phase Shift keying (PSK) to modulate both C/A and P-code onto the carrier. The other signal (known as the L2 carrier) is centered at 1227.60 MHz and uses PSK to modulate P-code onto the carrier. L1 carrier is the signal used by the commercial receivers. It is modulated with 1.023 MHz Pseudo-Random noise (PRN) code which is unique to each satellite. Each GPS satellite transmits the Navigation Message through C/A code. The C/A codes from at least four GPS satellites are required to calculate the user receiver position in Earth Centered Earth Fixed (ECEF) coordinate system (Gomes et al., 2007).

2.7.1. GPS Navigation Solution

It is stated earlier that minimum four GPS satellites are must be in view for the receiver to determine to 3-dimentional position (Fig.1). This is because there are four unknowns in the set of four navigation equations. Therefore, to solve for user position and time, we need to solve the following simultaneous equations Eq. (29) (Amaral et al, 2007, Gomes et al., 2007).

$$\begin{aligned}
\rho_1 &= \sqrt{(X_1 - x)^2 + (Y_1 - y)^2 + (Z_1 - z)^2} + c \cdot \Delta t \\
\rho_2 &= \sqrt{(X_2 - x)^2 + (Y_2 - y)^2 + (Z_2 - z)^2} + c \cdot \Delta t \\
\rho_3 &= \sqrt{(X_3 - x)^2 + (Y_3 - y)^2 + (Z_3 - z)^2} + c \cdot \Delta t \\
\rho_4 &= \sqrt{(X_4 - x)^2 + (Y_4 - y)^2 + (Z_4 - z)^2} + c \cdot \Delta t
\end{aligned} \tag{29}$$

ρ_1, ρ_2, ρ_3 and ρ_4 are the pseudo-ranges to each of the satellites. A pseudo-range is a measurement of the distance between the satellite and the receiver.
$X_i, Y_i; Z_i$ for i=1,2,3,4 are the coordinates of the satellites in the Earth Centered Earth Fixed, WGS-84 coordinate reference frame,
x, y, z are the receiver WGS-84 coordinates,
$c = 2.99792 \times 10^8$ (speed of light) m/s,
Δt is the receiver clock offset from GPS time (satellite time).

By linearizing Eq. (29) , one can get the observation vector (i.e. receiver position x, y, z) and clock bias Δt. GPS satellite sends data through navigation message in frames to GPS receiver. These data are in spherical coordinates and required to transform into Cartesian coordinates.

2.7.2. GPS satellite navigation message

The navigation message includes Almanac data, ephemeris data, timing data, ionospheric delay data and health data of the satellite. The information in the navigation message has basic five frames. Each frame is subdivided into five 300-bit sub-frames and has 10 words of 30 bit. Out of above mentioned frames, the Satellite Ephemeris data, ionospheric data frame and satellite timing data frame are of interest for the present work. A detailed description of all information contained in the navigation message is beyond the scope of this text.

The sub-frame of navigation message contains the ephemeris data, which is used to determine the precise satellite position and velocity required by the navigation solution. This ephemeris data is valid over a relatively short period of time (several hours), and applies only to the satellite transmitting it. The components of the ephemeris data are given in (Xu, 2007, Grewal et al., 2007).

2.7.3. Calculation of ECEF coordinates of the GPS satellite from Ephemeris data

The ephemeris data including the following elements will be extracted from navigation message and then further used to compute the GPS satellite position in the form of Earth Centered Earth Fixed (ECEF) coordinate frame using following formulas given in Eq. (30) as discussed in (Xu, 2007).

$a = \left(\sqrt{a}\right)^2$ Semimajor axis

$n_0 = \sqrt{\frac{\mu}{a^3}}$ Computed mean motion, rad/s

$M_k = E_k - e \sin E_k$ Kepler's equation of eccentric anomaly

$$f_k = \cos^{-1}\left(\frac{\cos E_k - 1}{1 - e\cos E_k}\right) \quad \text{True anomaly from cosine} \tag{30}$$

$E_k = \cos^{-1}\left(\frac{\mathrm{e} + \cos f_k}{1 + e\cos f_k}\right)$ Eccentric anomaly from cosine

With the help of above mentioned algorithm the k[th] GPS satellite position in ECEF coordinate frame is determined using Eq. (31).

$$\begin{aligned} X_k &= x_k \cos\Omega_k - y_k \cos i_k \sin\Omega_k && \text{ECEF X coordinate} \\ Y_k &= x_k \cos\Omega_k + y_k \cos i_k \cos\Omega_k && \text{ECEF Y coordinate} \\ Z_k &= y_k \sin i_k && \text{ECEF Z coordinate} \end{aligned} \tag{31}$$

Where x_k, y_k are the GPS satellite positions in the orbital frame. Eq. (31) converts satellite position from orbital frame to ECEF frame. A software routine for the same is developed in MATLAB.

3. RESULTS AND DISCUSSION

In this section the results obtained related to reference trajectory generation, least square orbit determination and EKF orbit determination method are discussed.

A. Reference trajectory generation

Software to generate reference trajectory is developed in MATLAB. The effect of various zonal perturbations like J_2, J_3 and J_4 were tested. The Keplerian model shown in Eq. (6) is numerically integrated with fixed step size Runge-Kutta 4[th] order method for the period of T=86,400 sec. Step size t =10 sec is used for orbit integration. As can be seen from Fig. 3, the satellite orbit is confined with its orbital plane i.e. under the influence of central gravitational field. The Eq. (7) is integrated first to get J_2 perturbation by neglecting J_3 and J_4 terms. As can be seen from Fig.4 when secular perturbation term J_2 is introduced, the satellite orbit gets deviated from the orbit in the central gravitation field.

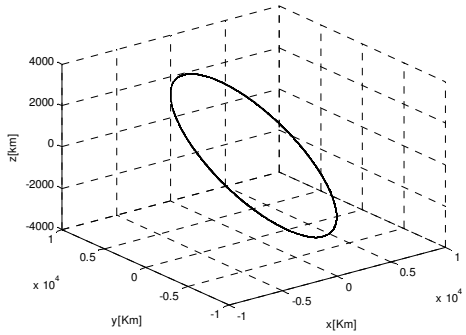

Figure: 3. Keplerian Orbit Integration

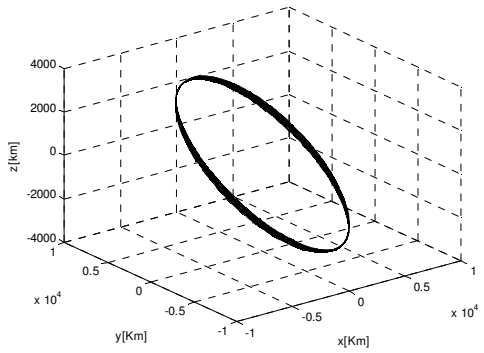

Figure: 4. Orbit Integration with J_2

To get the idea of the orbital parameter variation in detail each individual orbital parameter a (semimajor axis in km), e (eccentricity), i (inclination angle in degree), Ω(ascending node in degree), ω (argument of perigee in degree) respectively is plotted with respect to time separately. The Fig.5 shows orbital parameters variation with respect to time in Keplerian orbit. As can be seen from Fig. 5, there is no significant change in the orbital parameters except true anomaly (υ) (which define the angular position of orbiting body, it is subject to change with time due to the position changes) because there is no other force which causes the change in orbital parameters. The maximum and minimum values of orbital elements obtained in an orbit in different cases are given in Table 2. The variations in the orbital elements due to secular perturbations J_2, J_3 and J_4 are shown in Fig. 6. Satellite dynamic model Eq. (7) are then integrated considering the effects of J_2, J_3 and J_4 for the period T=86,400 sec with fixed step size=10 sec. As shown in Fig. 6d, the regression of the ascending node under the J_2, J_3 and J_4 perturbations is observed. In case of J_2, J_3 and J_4 perturbed orbit, the ascending node and argument of perigee exhibits significant almost linear variation. The motion of the ascending node occurs because of the added attraction of the Earth's equatorial bulge, which introduces force components towards the equator. The ascending node regresses for direct orbits ($0^0 < i < 90^0$) and advances for retrograde orbits ($90^0 < i < 180^0$). From this study it is observed that J_2 is the main zonal parameter which affects the state vector more. Other parameters like J_3 and J_4 have a greater impact for long term integration. In the present application the long term integration is not required.

Table 2: Variations in orbital elements

Orbital Parameters	**Keplerian orbit**		J_2		J_2, J_3 and J_4	
	Max.	Min.	Max.	Min.	Max.	Min.
a [km]	6828.956	6828.952	6828.975	6824.416	6871.082	6818.754
e	0.009016	0.009015	0.009311	0.00711	0.064504	0.007943
i [deg.]	28.47401	28.47401	28.47404	28.43975	28.5831	28.39334
Ω [deg.]	35.91182	35.91182	35.91182	28.96786	35.92338	29.04105
ω [deg.]	-44.5593	-44.5708	-32.5345	-58.0807	-0.00189	-46.7252

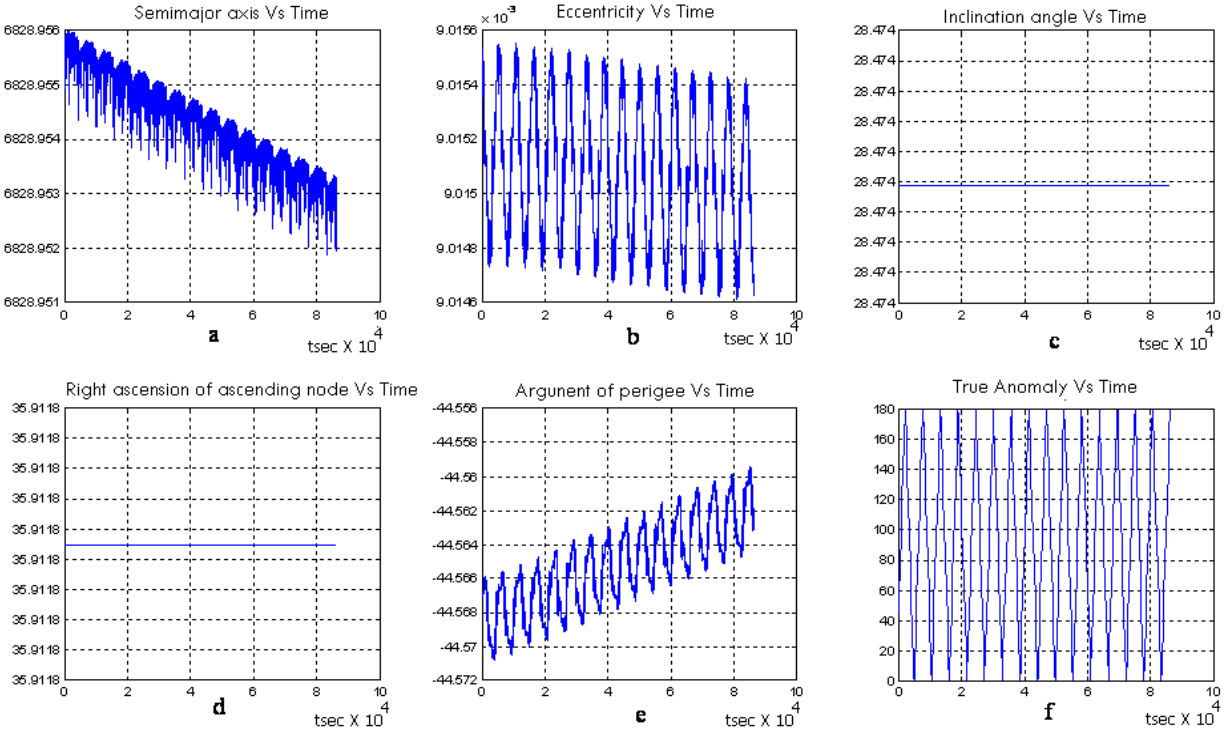

Figure 5. Orbital parameters variation in Keplerian orbit

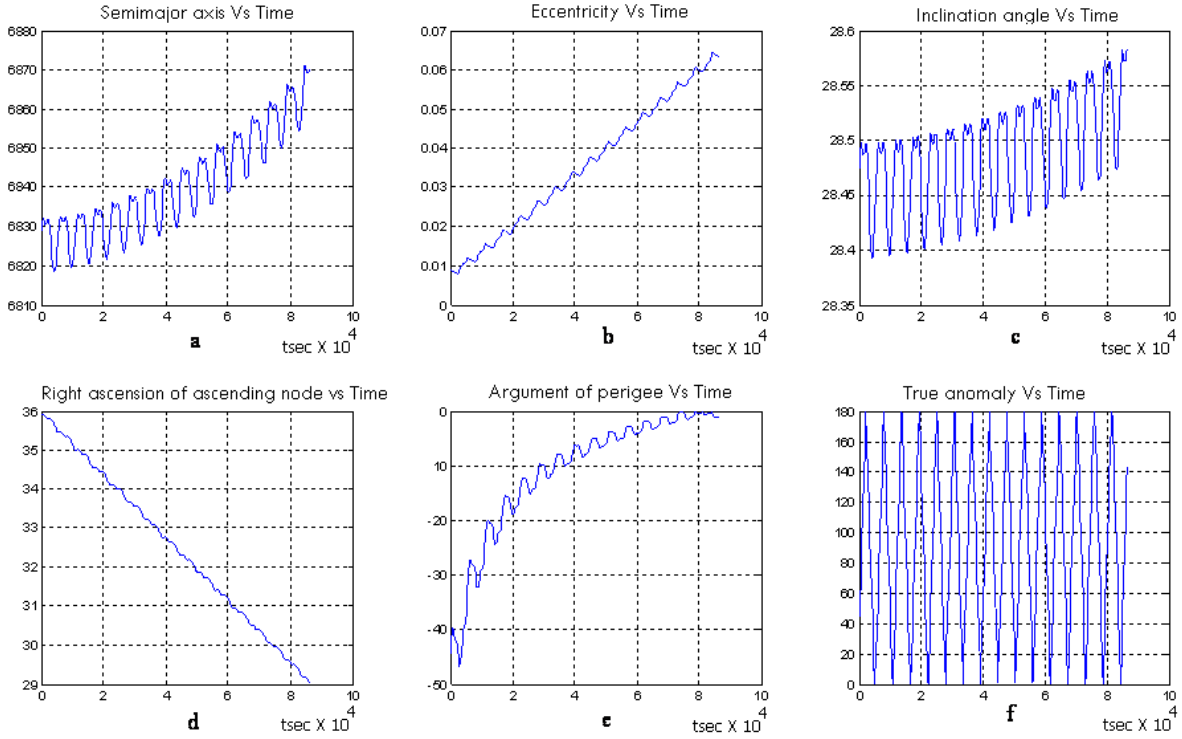

Figure 6. Orbital parameter variation due to main harmonic J_2, J_3 and J_4.

a. Atmospheric drag effect

The orbit of a satellite is integrated for a 1, 2 and 5 days period to test the effect of drag on the satellite orbital elements. It is observed from Fig. 7, that semimajor axis shows major declination with atmospheric drag effect. For longer time period i.e. for a period of 5 days semimajor axis decline by 500 meter (Fig 7e). This considerable declination in the semimajor axis affects the accuracy of the orbit determination.

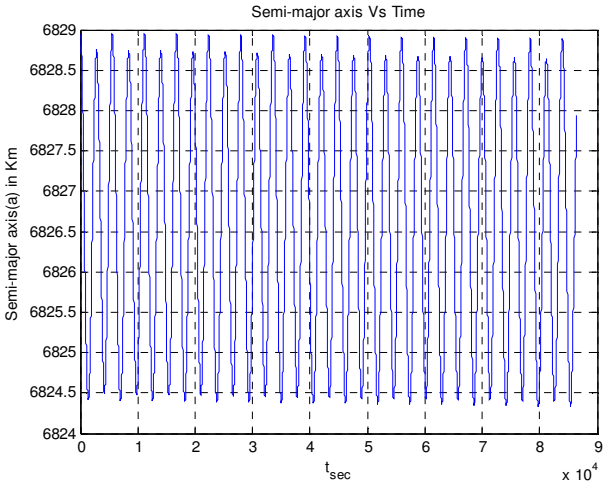

Fig: 7a. J_2 + Drag (Period: one day)

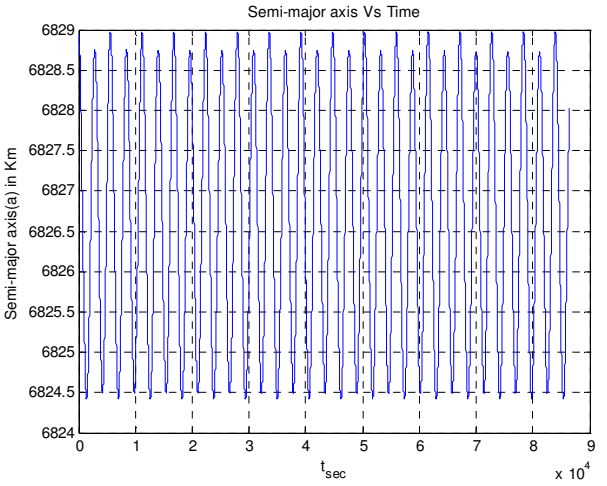

Fig: 7b. J_2 only (Period: one day)

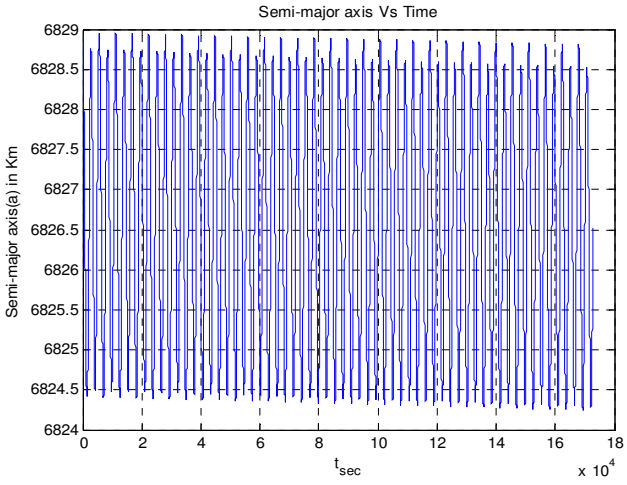

Fig: 7c. J_2 + Drag (Period: two day)

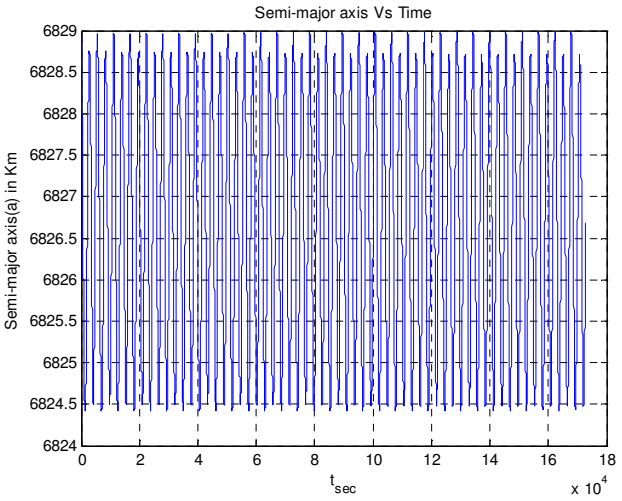

Fig: 7d. J_2 only (Period: two day)

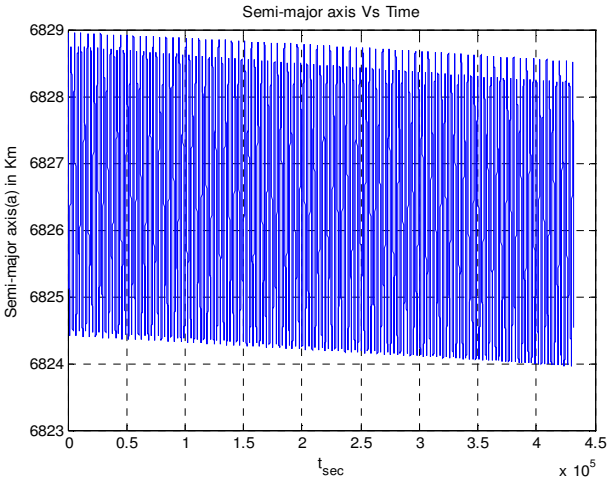

Fig: 7e. J_2 + Drag (Period: five day)

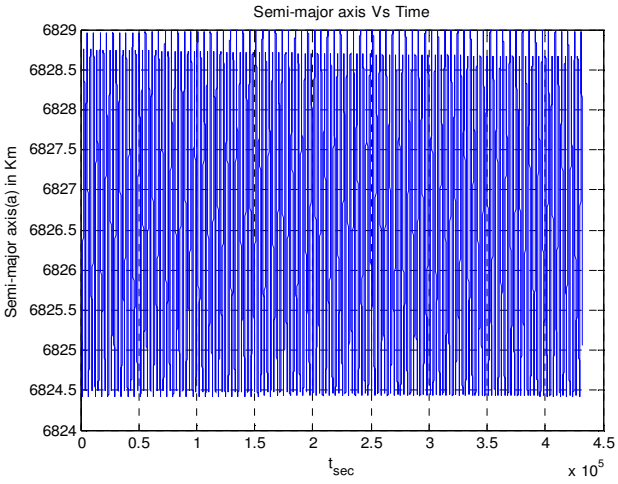

Fig: 7f. J_2 only (Period: five day)

B. Orbit estimation results: least squares

Least squares differential correction algorithm is used to determine the orbit of a spacecraft from simulation of position and velocity measurements generated along the reference trajectory. The subroutine for the same is developed in MATLAB environment. The true spacecraft position and velocity at initial epoch for present simulations with respect to the inertial reference frame of the standard epoch J2000.0 are given by;

$\vec{r}_0 = [3912.31743;\ -186.11297;\ 5913.91320]$ km; $\vec{v}_0 = [\ 5.925477;\ -2.525613;\ -3.988949]$ km/s.

The model equations used in this method are given in Eq. (7) and Eq. (18) to Eq. (22). Measurements are taken at 10-second intervals over a 100-second simulation. The measurement errors are zero-mean Gaussian with a standard deviation of the position measurement error given by $\sigma_{position}$ = 10 m, and a standard deviation of the velocity measurements given by $\sigma_{velocity}$ = 0.1 m/sec.

Table 3. Least square iterations for orbit estimation

Nr	Initial position components [km]			Initial velocity components [km/s]		
1	5482	1	1	1	1	1
2	2675.412	-4000.12	-1259.63	3.792749	4.888852	3.014527
3	4508.612	-7915.99	6013.159	4.330451	9.472996	-8.56845
4	2846.889	658.872	10627.15	9.703767	-6.5569	-13.5849
5	3523.785	-905.629	5868.684	7.235599	-0.69701	-4.03073
6	3919.372	-183.179	5974.346	5.880111	-2.54941	-4.24749
7	3913.082	-184.847	5914.523	5.906372	-2.54047	-3.98977

The estimated values of state vector components shown in Table 3, are in the agreement with the given true position and velocity components at initial epoch, at the level of a few hundred meters to one kilometer (position) and at the level of several tens of meters per second (velocity). In order to assess the performance of the least squares differential correction algorithm, the initial guesses for the position and velocity are given by $\vec{r}_0$ = [5482 1 1] km, and $\vec{v}_0$ = [1 1 1] km/sec. As can be seen from Table 3, the algorithm converges after seven iterations in the present case.

C. Orbit estimation: extended Kalman filter

The satellite dynamic model is of non-linear form. Due to the non-linear relation of the state vector and the measurements, multiple iterations are required to compute the state estimate. The subroutine for the same in developed in MATLAB environment. The true spacecraft position and velocity at the initial epoch for present simulations are given by;

$\vec{r}_0 = [3912.31743;\ -186.11297;\ 5913.91320]$ km; $\vec{v}_0 = [\ 5.925477;\ -2.525613;\ -3.988949]$ km/s.

Using EKF the reference trajectory is updated with each measurement. In the EKF method, the only analytical computations for the orbital EKF are the evaluations for the partial derivatives of dynamic model and observation model with respect to the state vector $\vec{x}$. These Jacobian, F, and sensitivity matrix H are evaluated at the current estimated state. Due to its sequential in nature it takes less iterations to compute state estimate.

Table 4. EKF iterations for orbit estimation

Nr	Position (km)			Velocity (km/sec)		
1	4156.668	265.6841	6260.527	-3.227	-19.4337	-14.3844
2	3911.886	-185.258	5913.071	5.94139	-2.54235	-3.97501
3	3911.886	-185.257	5913.072	5.941394	-2.54239	-3.97503

Therefore implementation of EKF algorithm is much more straightforward than Least Squares Differential Correction method. It is clearly seen from Table. 4, EKF converges much faster than least square method due to its sequential in nature.

4. CONCLUSIONS

In this work, the state vector is propagated using fixed step size orbit integration. Satellite orbit dynamic models with J_2, J_3 and J_4 are integrated. With this experiment, it is observed that orbit integration with J_2 only is sufficient to use for present application. Effect of atmospheric drag is also studied. Using the proposed simplified model it is concluded that it is feasible for on-board orbit determination application. To start the EKF orbit determination algorithm it is required to set the accurate initial guess. The same guess is determined first by least square algorithm and then it is further used in EKF orbit determination algorithm. Both, the least square and EKF orbit determination algorithms are developed and the results of the same are compared with each other. With our study it is observed that EKF algorithm is much faster than least square algorithm because of its recursive in nature and also shows comparable accuracy with least square method. This property of EKF algorithms makes it suitable for hardware implementation for autonomous orbit determination.

5. Acknowledgement

The authors thank the Indian Space Research Organization- University of Pune Space Technology Cell Pune, for the financial support ISAC Bangalore for technical support. The authors also thank Padmashree Pramod Kale for his valuable guidance and support.

REFERENCES

[1] Amaral J., Kuga H., Souza M., "Real time multisatellite orbit determination for constellation maintenance", Proceedings of COBEM. NAVSTAR GPS user equipment introduction, US Government, chapter 7, 2007.

[2] Bock H., Hugentobler U., Springer T, and Beutlerl G., "Efficient precise orbit determination of LEO satellites using GPS", Advances in Space Research,30(2), pp.295-300, 2002.

[3] Chiaradia A., Kuga H, and Prado A., "Onboard and Real-Time Artificial Satellite Orbit Determination Using GPS", Mathematical Problems in Engineering, Hindawi Publishing Corporation, 2013.

[4] Choi E., Yoon J., Lee B., Park S., Choi K.,"Onboard orbit determination using GPS observations based on the unscented Kalman filter",Advances in Space Research, 46,pp. 1440–1450, 2010,

[5] Degnan, J., and Pavlis, "Laser Ranging to GPS Satellites with Centimeter Accuracy", E.C.(1994):, GPS World, pp. 62-70, September, 1994.

[6] Gomes V., Kuga H., Chiaradia A., "Real-Time orbit determination solution using GPS Navigation Solution", J. Braz. Soc. Mech. Sci. & Eng., 29(3), pp. 274-278, 2007.

[7] Grewal M., Weill L., Andrews A., "Global Positioning System, Inertial Navigation and Integration", A John Wiley and Sons Inc, Publication, page.no 37, 2007.

[8] Pardal P., Kuga H, and deMoraes R., "Implications of the application of recursive least squares algorithms to satellite orbit determination using GPSmeasurements,"WSEAS Transactions on Systems, vol. 8, no. 3, pp. 334–343, 2009.

[9] Parkinson B., Spilker J., "Global Positioning System: theory and Applications", AIAA, Vol.1, Progress in Astronautics and Aeronautica 163, 1996.

[10] Taply B., Schutz B. and Born G, "Statistical orbit determination", Elsevier Academic Press, USA, 2004.

[11] Vallado D., McClain W., "Fundamentals of astrodynamics and applications", 3rd ed., Microcosm press, Ca,2007.

[12] Xu G., "GPS Theory, Algorithm and Applications", 2nd Edition, Springer, 2007.

[13] Yunck T., Bertiger W., Wu S., Bar-Sever Y., Christiansen E., Haines B., Lichten S., Muellerschoen R., and Willis P., "First Assessment of GPS-Based Reduced Dynamic Orbit Determination on TOPEX/Poseidon", Geophys. Res. Let., V.21, pp. 541-544, 1994.

[14] Zarchan P., " Fundamentals of Kalman Filtering: A Practical Approach", 2nd Edition, by , AIAA, 2005.

Received: 2014-01-15,

Reviewed: 2014-05-14, by A. Bobojć,

Accepted: 2014-05-16.